

Effect of Compatibilizer on Morphology, Thermal, and Rheological Properties of Polypropylene/Functionalized Multi-Walled Carbon Nanotubes Composite

Sang Hyun Jin,¹ Chang Heon Kang,¹ Kwan Han Yoon,¹ Dae Suk Bang,¹ Young-Bin Park²

¹Department of Polymer Science and Engineering, Kumoh National Institute of Technology, Gumi, Gyeongbuk 730-701, Korea

²Department of Industrial and Manufacturing Engineering, FAMU-FSU College of Engineering, Tallahassee, Florida 32310-6046

Received 29 August 2007; accepted 24 July 2008

DOI 10.1002/app.29009

Published online 17 October 2008 in Wiley InterScience (www.interscience.wiley.com).

ABSTRACT: Multi-walled carbon nanotubes (MWCNTs) filled polypropylene (PP) composites were prepared by a corotating intermeshing twin screw extruder. To improve the dispersion of MWCNTs, the surface of MWCNT was modified with 1,10-diaminododecane, and maleic anhydride grafted polypropylene (MA-g-PP) was used as a compatibilizer. Micrographs of well dispersed functionalized MWCNTs (diamine-MWCNT) were observed due to the reaction between MA-g-PP and diamine-MWCNT in PP/MA-g-PP/diamine-MWCNTs composites. The different

behaviors in crystallization and melting temperatures of PP/MA-g-PP/diamine-MWCNTs composite were observed compared to PP and PP/neat-MWCNT. Especially, the decomposition temperature of the composite was increased by 50°C compared to PP. PP/MA-g-PP/diamine-MWCNTs composite showed the highest complex viscosity. © 2008 Wiley Periodicals, Inc. *J Appl Polym Sci* 111: 1028–1033, 2009

Key words: polypropylene; nanocomposites; compatibilization; morphology; rheology

INTRODUCTION

Carbon nanotubes (CNTs) have been used as extremely strong nano-reinforcements for composites, which possess extraordinarily high strength with low weight and moderate electrostatic discharge properties.¹ However, the application of CNTs for composites has been largely hampered by their poor dispersion in polymer resin and weak interfacial bonding with polymer matrix.² To achieve optimal enhancement in the properties of CNT/polymer composites, chemical modification of the CNT surface has been used. Recently, the influence of the functionalized CNTs on the properties of poly(methyl methacrylate) (PMMA),³ epoxy,⁴ polyamide,⁵ polyimide,⁶ and poly(ethylene terephthalate)^{7–9} was studied. These results indicated that functionalization led to good dispersion in polymer matrix and showed improved mechanical properties due to the improved interaction between the functionalized nanotubes and the polymer matrix.

Among the most versatile polymer matrices, polypropylene (PP) is a thermoplastic having a higher consumption because of their well-balanced physical and mechanical properties and their easy processability at a relatively low cost. Recently, the study of PP/CNT composites demonstrated the results of crystallization,^{10–12} electrical resistivity,^{11,13} thermal, and flammability,¹⁴ mechanical properties¹⁵ and morphology.^{16–18} In their works, the crystallization rate of the composites increased with the addition of CNTs. The electrical percolation threshold was obtained at 2 wt % of CNT. The morphology indicated that the dispersion of CNTs in the PP matrix was not very perfect even at the low content of 0.5 wt %. At high CNT content of 5 or 10 wt %, it was found that approximately micrometer diameter clusters of CNTs appeared in localized areas.

In this study, we prepared the surface modified multi-walled carbon nanotube (diamine-MWCNT) to improve the dispersion of MWCNTs in the PP matrix. Also, to improve the interfacial interaction between the surface modified multi-walled carbon nanotube and PP, maleic anhydride grafted polypropylene (MA-g-PP) was used as a compatibilizer in PP/diamine-MWCNT composites. The amount of MA-g-PP and MWCNTs used for the composites was 10 and 2 wt % based on the PP, respectively.

Correspondence to: K. H. Yoon (khyoon@kumoh.ac.kr).

Contract grant sponsor: New University for Regional Innovation.

EXPERIMENTAL

Materials

Multi-walled carbon nanotubes (MWCNTs) used in this work were manufactured by chemical vapor deposition (CVD) process and supplied from Iljin Nanotech (Inchon, Korea). Nitric acid and sulfuric acid were obtained from Junsei (Tokyo, Japan). *N,N*-dimethyl formamide (DMF) and 1,10-diaminodecane were obtained from Aldrich (Yongin, Korea) to prepare surface modified-MWCNT. Polypropylene (PP) and maleic anhydride grafted polypropylene (MA-g-PP) were supplied from Hyosung (Ulsan, Korea) and Honam Petrochem (Oaejeon, Korea), respectively. Maleic anhydride (MAH) content in MA-g-PP was 10 wt %.

Preparation of surface modified-MWCNT

Neat-MWCNTs were mixed with sulfuric and nitric acids for 5 min, and then sonicated for dispersion for 1 h. The mixture was refluxed for 12 h at 110°C. Acid-MWCNTs were obtained by washing and filtering the mixture with distilled water and then drying in a freeze drier. The acid-MWCNT solution was mixed again with 1,10-diaminodecane (DA10) at 100°C for 48 h. The mixture was reacted vigorously after 5–10 min. The unreacted DA10 was removed from the reaction mixture with distilled water. The solution obtained was quenched at –84°C for 6 h, and then dried in a freeze drier for 5 days. The product obtained was diamine-MWCNTs. The schematic of the reaction procedure is shown in Figure 1.

Preparation of the nanocomposites

Prior to melt processing, all of the compounds were mixed by ball mill in advance. The composites were prepared by an intermeshing corotating twin screw extruder. During extrusion, compounding was carried out using a screw rotating speed of 100 rpm and a temperature profile of 150, 180, 200, 200, 200, 200, and 200°C from the hopper to the die for the sequential heating zones. After compounding, the material was extruded from a die, which had two cylindrical nozzles of 4-mm diameter, to produce cylindrical extrudates. These were immersed immediately in a water bath (20°C) and pelletized with an adjustable rotating knife into 5-mm pellets.

Measurements

The infrared spectra of neat-MWCNT, acid-MWCNT, and diamine-MWCNT were recorded using a Fourier transform infrared spectrometer (FTIR-300E, Jasco).

The thermal behavior of the PP/MWCNT composites was characterized using a DuPont 910 differen-

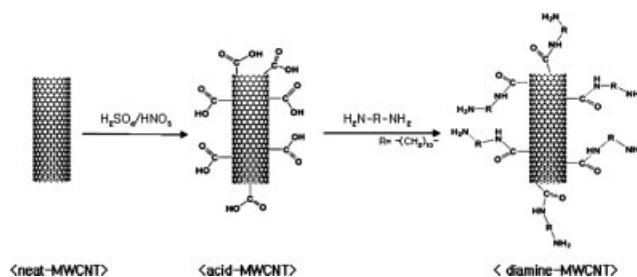


Figure 1 Schematic representation of the formation of acid-MWCNTs and diamine-MWCNTs.

tial scanning calorimetry (DSC). The melting and crystallization temperatures were determined at heating and cooling rates of 20°C min⁻¹. The thermal stability of the samples was measured by thermogravimetric analysis (TGA) using a TA Instruments 2950 thermogravimetric analyzer. Mass loss was traced as samples were heated at a rate of 10°C min⁻¹ from room temperature to 700°C under nitrogen.

Dynamic rheological measurements were performed using a rotational rheometer (PHYSICA Rheo-Lab MC120). The measurements were carried out in an oscillatory shear mode using the parallel plate geometry. Prior to any measurement, all samples were allowed to relax at the measuring temperature for 2 min and then sheared at a low shear rate (0.01 s⁻¹) for 3 min under a nitrogen atmosphere. Frequency sweeps were performed from 0.1~100 rad s⁻¹. A strain sweep was carried out to determine the strain limit for linear viscoelastic responses. A strain of 5% was applied during the measurement, which was below the limit for linear viscoelastic responses.

Morphology of the composites was examined by scanning electron microscopy (SEM, S-4300, Hitachi).

RESULTS AND DISCUSSION

Fourier transform infrared spectroscopy

FTIR was employed to characterize chemically modified carbon nanotubes. The FTIR spectra of neat-MWCNT, acid-MWCNT, and diamine-MWCNT are shown in Figure 2. The peaks at 1721 and 1176 cm⁻¹ are in correspondence with C=O and C–O stretching, respectively, indicating the existence of carboxyl groups in acid-MWCNTs. In the diamine-MWCNT spectrum, the peak at 1721 cm⁻¹ (C=O stretching) are observed, however, that at 1176 cm⁻¹ (C–O stretching) no longer exists. This is in accordance with the schematic of the end product after the reaction with DA10 shown in Figure 1. Diamine functionalization is further evidenced by the characteristic peaks that represent

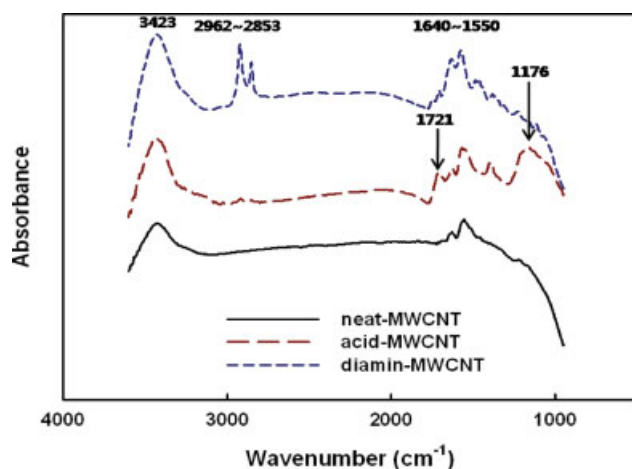


Figure 2 FTIR spectra of neat-MWCNTs, acid-MWCNTs and diamine-MWCNTs. [Color figure can be viewed in the online issue, which is available at www.interscience.wiley.com.]

$\text{—CH}_2\text{—}$ stretching ($2853\sim 2926\text{ cm}^{-1}$) and N—H bending ($1550\sim 1640\text{ cm}^{-1}$).

To confirm the reaction between MA-g-PP and diamine-MWCNT during melt mixing, FTIR spectra of MA-g-PP, diamine-MWCNT and MA-g-PP/diamine-MWCNT composite were measured and are shown in Figure 3 in the range $2000\text{--}1500\text{ cm}^{-1}$. In MA-g-PP spectrum, the peaks at 1863 cm^{-1} (C=O asymmetric stretching) and at 1780 and 1715 cm^{-1} (C=O symmetric stretching) are observed. In MA-g-PP/diamine-MWCNT composite, N—H bending ($1550\sim 1640\text{ cm}^{-1}$) in diamine-MWCNT disappeared. It indicates that the reaction between MA-g-PP and diamine-MWCNT occurred during melt mixing.

The morphology of PP/MWCNTs composites

Figure 4 shows the field-emission scanning electron micrographs of the PP/neat-MWCNT, PP/MA-g-PP/neat-MWCNT, PP/diamine-MWCNT, and PP/MA-g-PP/diamine-MWCNT composites. For PP/neat-MWCNT composite, it is clear from the micrograph that the dispersion of neat-MWCNT in the PP matrix is not perfect [Fig. 4(a,b)]. In some areas the concentration of neat-MWCNTs is high, but none of neat-MWCNTs can be found in other areas. Approximately micrometer diameter clusters of neat-MWCNTs appear in some areas, where the nanotubes are entangled together. This can be ascribed to the strong intermolecular van der Waals interactions among nanotubes. Addition of MA-g-PP to PP/neat-MWCNTs composite shows slightly different morphology [Fig. 4(c,d)]. In contrast to PP/neat-MWCNT composite, no micrometer clusters are observed, but neat-MWCNTs are agglomerated in some areas, which may be MA-g-PP matrix. Individ-

ual nanotubes are not distinguished in PP/neat-MWCNTs composite, but in PP/MA-g-PP/neat-MWCNTs composite, those are clearly seen due to the MA-g-PP. For PP/diamine-MWCNTs composite, there are still some areas where none of diamine-MWCNTs can be found, but the diamine-MWCNTs, which have been obtained from the reaction between acid-MWNTs and DA10, is characterized by a lower degree of aggregation as compared to neat-MWCNTs [Fig. 4(e)]. The lower degree of aggregation in functionalized MWCNTs is attributed not only to the functional groups, such as carboxyl and diamine, but also to their shorter lengths. The effect of MA-g-PP for the dispersion of nanotubes in the PP matrix is quite clear in PP/MA-g-PP/diamine-MWCNTs composite [Fig. 4(f)]. Well-dispersed micrograph of diamine-MWCNT is observed due to the strong interfacial interaction between MA-g-PP and functionalized MWCNTs although there are still some areas where diamine-MWCNTs are not found. Pires et al.¹⁹ corroborated the imide linkage between the amino end groups of polyamide-6 and the carboxylic groups of MA-g-PP which resulted in the formation of the interfacial layer.

Thermal properties of PP/MWCNTs composites

Figure 5 shows the DSC curves of PP, MA-g-PP, and PP/MWCNT composites. Polypropylene crystallized at 116°C , while crystallization in PP/MA-g-PP blend occurred at 114°C . The crystallization peak temperatures of the composites show the positive effect of nanotubes on the crystallization rate of PP regardless of neat-MWCNT or diamine-MWCNT. It suggests that nanotubes act as nucleating sites for PP crystallization. It can be also explained with the crystallite size. Zhang et al.¹⁸ reported that the spherulite size

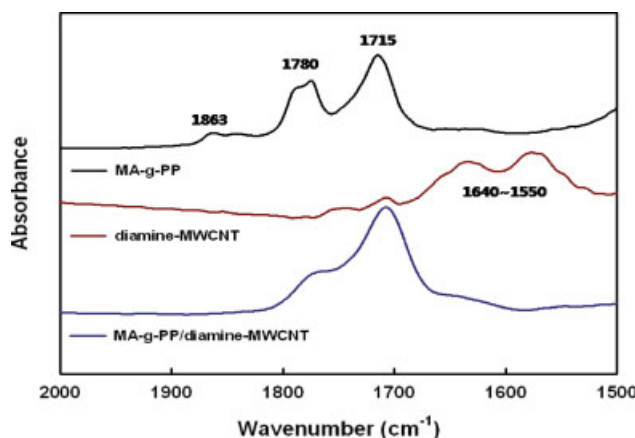


Figure 3 FTIR spectra of MA-g-PP, diamine-MWCNTs and MA-g-PP/diamine-MWCNT composite. [Color figure can be viewed in the online issue, which is available at www.interscience.wiley.com.]

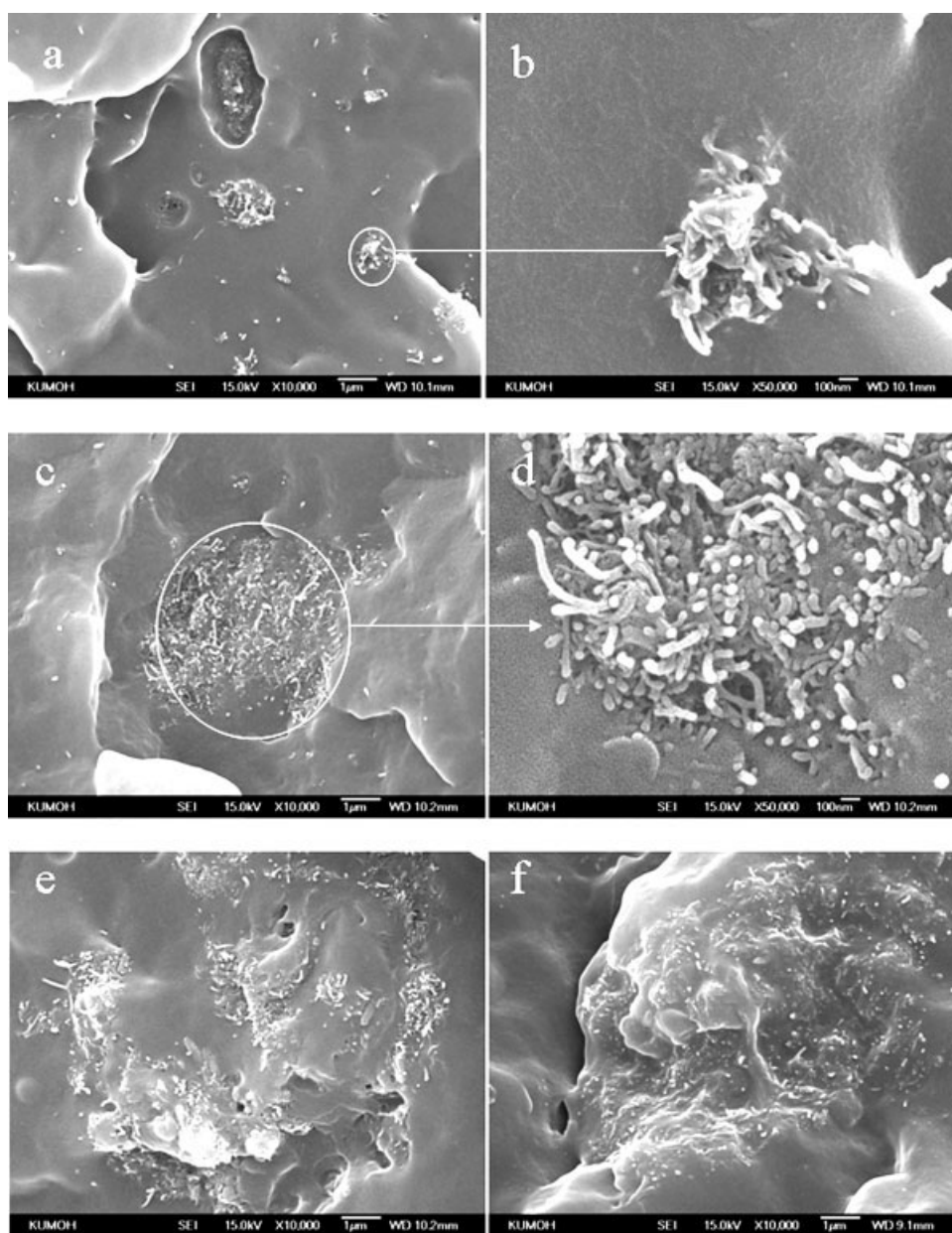


Figure 4 SEM micrographs of PP/neat-MWCNT (a,b), PP/MA-g-PP/neat-MWCNT (c,d), PP/diamine-MWCNT (e), and PP/MA-g-PP/diamine-MWCNT (f).

in PP/MWCNT composites was much smaller than in PP, resulting in the increase in crystallization rate. However, the crystallization peak temperature of PP/MA-g-PP/diamine-MWCNT composite is low compared to the other composites. The low crystallization temperature of PP/MA-g-PP/diamine-MWCNT composite may arise from large spherulite size resulting from the reaction between amino end groups of diamine-MWCNT and carboxylic groups of MA-g-PP. It can be shown in melting peak temperature of PP/MA-g-PP/diamine-MWCNT composite [Fig. 5(b)]. Polypropylene melts at 165°C, while melting in PP/MA-g-PP blend occurred at 163°C. The melting temperatures of PP/MWCNT

composites correspond to PP except for PP/diamine-MWCNT composite of which the melting temperature is slightly higher than that of PP.

Figure 6 shows the TGA curves of PP, MA-g-PP, and PP/MWCNT composites. The decomposition temperatures were measured at 5 wt % of weight loss. The decomposition temperature of PP appears at 335°C, and that of the composites is significantly increased by 30~50°C. The results indicate that the addition of nanotubes significantly enhanced the thermal stability of PP. The increased decomposition temperature of the composites can be explained by physical-chemical adsorption of the decomposed products. Yang et al.¹⁷ suggested that the increase in

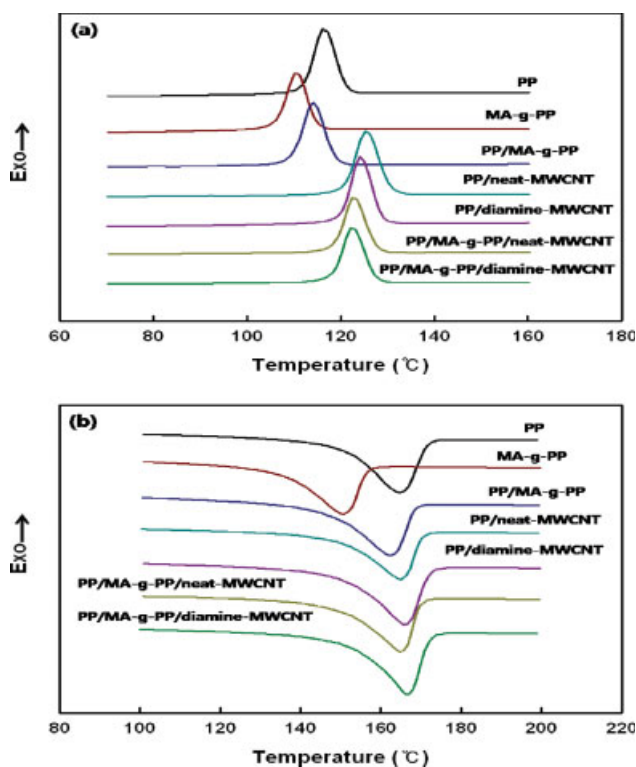


Figure 5 The DSC curves of PP, MA-g-PP, PP/MA-g-PP and its composites with neat-MWCNT and diamine-MWCNT; (a) cooling scans, (b) heating scans. [Color figure can be viewed in the online issue, which is available at www.interscience.wiley.com.]

decomposition temperature of PP/MWCNT composite was mainly attributed to the strong physical adsorption of PP molecules on the nanotube surfaces. The adsorbed molecules are much less active than those far from the nanotube surface, and thus volatilization is delayed. The increase in decomposi-

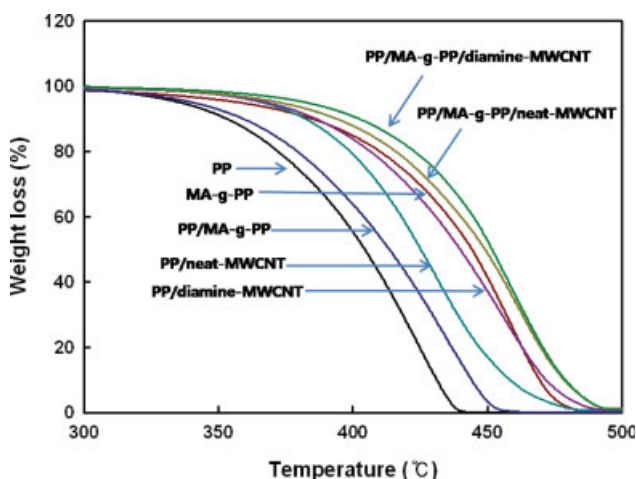


Figure 6 TGA overlay for PP, MA-g-PP, PP/MA-g-PP and its composites with neat-MWCNT and diamine-MWCNT. [Color figure can be viewed in the online issue, which is available at www.interscience.wiley.com.]

TABLE I
Thermal Properties of PP, MA-g-PP, and PP/MWCNT Composites

Samples	T_m (°C) ^a	T_c (°C) ^a	T_d (°C) ^b
PP	165	116	335
MA-g-PP	150	110	357
PP/MA-g-PP	163	114	340
PP/neat-MWCNT	165	125	366
PP/diamine-MWCNT	165	124	369
PP/MA-g-PP/neat-MWCNT	165	124	373
PP/MA-g-PP/diamine-MWCNT	167	122	383

^a Peak temperatures of melting and crystallization.

^b Values at measured 5 wt % of weight loss.

tion temperature for the composites except for PP/MA-g-PP/diamine-MWCNT composite can be explained by physical adsorption. However, the decomposition temperature of PP/MA-g-PP/diamine-MWCNT composite is highest among the composites. The largest increase of the composite cannot be explained by only physical adsorption since chemical modification was made to nanotubes and MA-g-PP was used as a compatibilizer. So the significant increase in thermal stability of PP/MA-g-PP/diamine-MWCNT composite is attributed to chemical adsorption of MA-g-PP on the diamine-MWCNT surfaces as well as physical adsorption. The melting, crystallization peak temperatures, and decomposition temperatures of PP, MA-g-PP and PP/MWCNT composites are listed in Table I.

Rheological properties of PP/MWCNTs composites

Figure 7 shows the frequency dependence of complex viscosity of PP, MA-g-PP, PP/MA-g-PP, and PP/MWCNTs composites. The complex viscosities were measured at 190°C. It is clearly seen that the

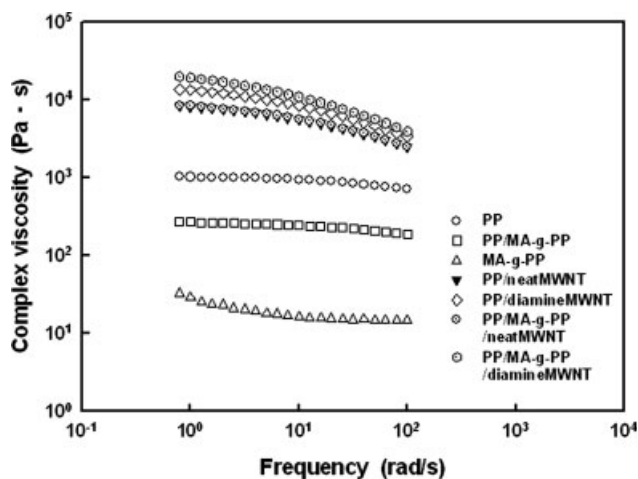


Figure 7 Complex viscosities of PP, MA-g-PP, PP/MA-g-PP, and its composites with neat-MWCNT and diamine-MWCNT.

addition of nanotubes to PP leads to an increase in complex viscosity. However, the magnitudes of viscosity enhancement are quite different. The PP showed Newtonian behavior in the experimental frequency ranges, as evidenced by nearly constant viscosity, and the viscosity of the composites increased in the order of neat-MWCNT, MA-g-PP/neat-MWCNT, diamine-MWCNT, and MA-g-PP/diamine-MWCNT composites as shown in Figure 7. The viscosity of composites deviates from Newtonian behavior and exhibits a very strong shear thinning effect. The viscosity value of PP/diamine-MWCNT composite is higher than that of PP/neat-MWCNT composite. It indicates that the dispersion of diamine-MWCNT in PP matrix is better than that of neat-MWCNT, effectively preventing PP from flowing. It is interesting to see the viscosity of the composites containing MA-g-PP. MA-g-PP has the lowest viscosity value in this study. If there is no interaction between MA-g-PP and neat-MWCNT, the viscosity value of the PP/MA-g-PP/neat-MWCNT composite should be decreased compared to PP/neat-MWCNT composite. However, there is no difference in viscosity between two composites. It suggests that MA-g-PP is more compatible with neat-MWCNT than PP, which has been confirmed by the morphology [Fig. 4(a-c)]. The effect of MA-g-PP is clearly seen in PP/MA-g-PP/diamine-MWCNT composite, which has the highest viscosity value. The reaction between amide end groups in diamine-MWCNTs and carboxylic groups in MA-g-PP was confirmed to make new copolymer at the interface.¹⁷ It suggests that the increase in viscosity of the composite arises from the reaction. Our previous paper⁸ demonstrated that the increase in the viscosity of PET/functionalized MWCNT composite resulted from the partial crosslinking between PET and functionalized MWCNT. Similarly, the reaction between MA-g-PP and diamine-MWCNTs may be partial crosslinking.

CONCLUSIONS

Polypropylene (PP)/multi-walled carbon nanotube (MWCNT) composites were prepared by industry-scale extrusion. To improve the dispersion of MWCNTs, the surface of MWCNT was modified with 1,10-diaminodecane and maleic anhydride

grafted polypropylene (MA-g-PP) was used as a compatibilizer. Approximately micrometer diameter clusters of neat-MWCNTs appeared in partial areas and neat-MWCNTs were entangled together whereas functionalized MWCNTs were relatively disentangled in the PP matrix. PP/MA-g-PP/diamine-MWCNT composite showed a fine dispersion of diamine-MWCNT due to the strong interfacial interaction between MA-g-PP and functionalized MWCNTs. The compatibilizing effect of MA-g-PP was well seen in thermal stability and complex viscosity of the composite, in which the highest thermal decomposition temperature and complex viscosity were observed.

References

1. Lau, K. T.; Hui, D. *Carbon* 2002, 40, 1605.
2. Chen, Q.; Dai, L.; Gao, M.; Huang, S.; Mau, A. *J Phys Chem B* 2001, 105, 618.
3. Wang, M.; Pramoda, K. P.; Goh, S. H. *Carbon* 2006, 44, 613.
4. Gojny, F. H.; Nastalczyk, J.; Roslaniec, Z.; Schulte, K. *Chem Phys Lett* 2003, 370, 820.
5. Zhao, D.; Hu, G.; Justice, R.; Schaefer, D.W.; Zhang, S.; Han, C. C. *Polymer* 2005, 46, 5125.
6. Zhu, B. K.; Xie, S. H.; Xu, Z. K.; Xu, Y. Y. *Compos Sci Technol* 2006, 66, 548.
7. Shin, D. H.; Yoon, K. H.; Kwon, O. H.; Min, B. G.; Hwang, C. I. *J Appl Polym Sci* 2006, 99, 900.
8. Jin, S. H.; Park, Y. B.; Yoon, K. H. *Compos Sci Technol* 2007, 67, 3434.
9. Jin, S. H.; Yoon, K. H.; Park, Y. B.; Bang, D. S. *J Appl Polym Sci* 2008, 107, 1163.
10. Bhattacharyya, A. R.; Sreekumar, T. V.; Liu, T.; Kumar, S.; Ericson, L. M.; Haugr, R. H.; Smalley, R. E. *Polymer* 2003, 44, 2373.
11. Seo, M. K.; Lee, J. R.; Park, S. *J Mater Sci Eng A* 2005, 404, 79.
12. Leelapornpisit, W.; Ton-That, M. T.; Perrin-Sarazin, F.; Cole, K. C.; Denault, J.; Simard, B. *J Appl Polym Sci Part B Polym Phys* 2005, 43, 2445.
13. Seo, M. K.; Park, S. *J Chem Phys Lett* 2004, 395, 44.
14. Kashiwagi, T.; Grulke, E.; Hilding, J.; Groth, K.; Harris, R.; Butler, K.; Shields, J.; Kharchenko, S.; Douglas, J. *Polymer* 2004, 45, 4227.
15. López Manchado, M. A.; Valentini, L.; Biagiotti, J.; Kenny, J. M. *Carbon* 2005, 43, 1499.
16. Valentini, L.; Biagiotti, J.; Kenny, J. M.; Santucci, S. *Compos Sci Technol* 2003, 63, 1149.
17. Yang, J.; Lin, Y.; Wang, J.; Lai, M.; Li, J.; Liu, J.; Tong, X. *J Appl Polym Sci* 2005, 98, 1087.
18. Zhou, Z.; Wang, S.; Zhang, Y.; Zhang, Y. *J Appl Polym Sci* 2006, 102, 4823.
19. Roeder, J.; Oliveira, R. V. B.; Goncalves, M. C.; Soldi, V.; Pires, A. T. N. *Polymer Test* 2002, 21, 815.